Lipid microenvironment affects the ability of proteoliposomes harboring TNAP to induce mineralization without nucleators

Ana Maria Sper Simão[#1], **Maytê Bolean**[#1], **Bruno Zoccaratto Favarin**[1], **Ekeveliny Amabile Veschi**[1], **Camila Bussola Tovani**[1], **Ana Paula Ramos**[1], **Massimo Bottini**[2,3], **Rene Buchet**[4,5,6,7,8], **José Luis Millán**[3], and **Pietro Ciancaglini**[1]

[1]Departamento de Química, Faculdade de Filosofia, Ciências e Letras de Ribeirão Preto da Universidade de São Paulo (FFCLRP-USP), Av. Bandeirantes 3900, Ribeirão Preto, SP 14040-901, Brazil

[2]Department of Experimental Medicine and Surgery, University of Rome Tor Vergata, 00133 Rome, Italy

[3]Sanford Burnham Prebys Medical Discovery Institute, La Jolla, CA 92037, USA

[4]UFR Chimie Biochimie, Universite Lyon 1, 69 622 Villeurbanne Cedex, France

[5]ICBMS, UMR 5246, CNRS, 69 622 Villeurbanne Cedex, France

[6]INSA, Lyon, 69 622 Villeurbanne Cedex, France

[7]CPE, Lyon, 69 622 Villeurbanne Cedex, France

[8]Universite de Lyon, 69 622 Villeurbanne Cedex, France

[#] These authors contributed equally to this work.

Abstract

Tissue-nonspecific alkaline phosphatase (TNAP), a glycosylphosphatidylinositol-anchored ectoenzyme present on the membrane of matrix vesicles (MVs), hydrolyzes the mineralization inhibitor inorganic pyrophosphate as well as ATP to generate the inorganic phosphate needed for apatite formation. Herein, we used proteoliposomes harboring TNAP as MV biomimetics with or without nucleators of mineral formation (amorphous calcium phosphate and complexes with phosphatidylserine) to assess the role of the MVs' membrane lipid composition on TNAP activity by means of turbidity assay and FTIR analysis. We found that TNAP-proteoliposomes have the ability to induce mineralization even in the absence of mineral nucleators. We also found that the addition of cholesterol or sphingomyelin to TNAP-proteoliposomes composed of 1,2-dipalmitoyl-*sn*-glycero-3-phosphocholine reduced the ability of TNAP to induce biomineralization. Our results suggest that the lipid microenvironment is essential for the induction and propagation of minerals mediated by TNAP.

Keywords

Biomineralization; Proteoliposome; Alkaline phosphatase; Matrix vesicles; Nucleational core

Introduction

During bone formation, osteoblasts or chondrocytes produce and mineralize the extracellular matrix (ECM) [1]. The formation of apatite is initiated in the lumen of matrix vesicles (MVs) and has been described to depend on the presence of a nucleator, the nucleational core (NC), in the lumen of MVs [2, 3]. The components of the NC, the amorphous calcium phosphate (ACP) in association with phosphatidylserine (PS), result in calcium–phosphate–lipid complexes (PS-CPLXs). Further accumulation of Ca^{2+} and inorganic phosphate (P_i) in MVs can lead to the growth of apatite crystals, which then propagate on the ECM and continue to grow onto collagenous fibers, forming bone tissues. Tissue-nonspecific alkaline phosphatase (TNAP, E.C. 3.1.3.1) [4, 5] is a glycosylphosphatidylinositol (GPI)-anchored protein present on the plasma membrane of osteoblasts and chondrocytes, and also on the surface of MVs [6]. TNAP provides P_i needed for apatite crystallization by hydrolyzing phosphomonoesters [7]. Among various substrates, TNAP catalyzes the hydrolysis of pyrophosphate (PP_i), a mineralization inhibitor [8], thus facilitating the formation of apatite crystals [5, 9–11]. Adequate local concentrations of extracellular PP_i, originating from the hydrolysis of sodium adenosine-5′-triphosphate (ATP) by nucleotide pyrophosphatases/phosphodiesterases (NPPs) or from transport of intracellular PP_i by the action of progressive ankylosis protein (ANK), and of extracellular P_i originating from the hydrolysis of PP_i or of other phosphomonoesters by TNAP are essential to allow normal mineralization [5, 12–14]. The catalytic properties of the GPI-anchored, polidocanol-solubilized and phosphatidylinositol-specific phospholipase C-released TNAP suggest that the location of TNAP on the membrane of MVs can control substrate selectivity in this micro-compartment, suggesting that assays of TNAP bound to MVs or bound to proteoliposomes might be more relevant than assays performed with solubilized enzymes, particularly when studying the hydrolysis of organophosphate substrates [15].

The MVs' membrane contains high content of cholesterol (Chol), sphingomyelin (SM) and PS, resembling the lipid content of rafts in the plasma membrane [16, 17]. The organization of the lipids influences the activity of the proteins present on the rafts, thus the study of the interactions between TNAP and the lipids of the MVs' membrane is essential to understand the initiation and propagation of biomineralization process [18–21].

The ability of proteoliposomes to mimic the function and structure of biomembranes [22–27] makes them a convenient model to determine the factors of MV-mediated mineralization. Other researchers also aim to work with therapeutic mimetic cell to provide a source of cell-like assemblies, which exhibits the core structural or functional properties of their natural counterparts with broad envisioned applications in biomedicine. One most recent example is the generation of microreactors loaded with liposomes harboring TNAP to biomineralization studies [28].

Our research group has standardized a methodology to fabricate biomimetic models of MVs containing TNAP incorporated into lipid microdomains, allowing biochemical and biophysical studies of the biomineralization driven by MVs [22, 29, 30]. Here, we prepared proteoliposomes harboring TNAP composed by 1,2-dipalmitoyl-*sn*-glycero-3-phosphocholine (DPPC), DPPC:Chol (9:1), DPPC:SM (9:1) and DPPC:Chol:SM (8:1:1) (molar ratios) to evaluate how the lipid composition affects the ability of proteoliposomes to form apatite minerals through the activity of TNAP for the biological substrate ATP as the source of P_i when incubated in a synthetic cartilage lymph (SCL) buffer either in the presence or absence of nucleators.

Materials and methods

Production of TNAP

Human TNAP was expressed as previously described [24, 31] and used immediately after detergent removal to avoid aggregation.

Liposome preparation

DPPC, DPPC:Chol (9:1), DPPC:SM (9:1), and DPPC:Chol:SM (8:1:1) (molar ratios) were prepared in 50 mM Tris–HCl buffer, pH 7.5, containing 2 mM $MgCl_2$, to yield a final solution with 10 mg/mL of lipids, as previously described [30].

Proteoliposome preparation

TNAP (0.02 mg/mL) was incorporated into the liposomes dispersed in a 50 mM Tris–HCl buffer, pH 7.5, containing 2 mM $MgCl_2$ by direct insertion in a 1:10,000 protein:lipid (molar ratio). The mixture was incubated at 25 °C for 1 h and ultracentrifuged at $100,000 \times g$ for 1 h, at 4 °C. The pellet (proteoliposomes) was resuspended to the original volume in the same buffer. The activity of TNAP in both pellet and supernatant was assayed to determine the percentage of TNAP incorporation into liposomes [29]. The protein concentrations were estimated as described by Hartree [32] in the presence of 2% (0.2 g/mL) SDS. Bovine serum albumin was used as a standard.

Dynamic light scattering measurement

The determination of liposomes and proteoliposomes' size distribution was performed by dynamic light scattering (DLS) as previously described [26]. Average values ($n = 5$) of the vesicles' diameters was obtained at 25 °C by unimodal distribution, previously filtered (0.8 mm). DLS measurements were performed throughout the period of use of the samples (7 days) and both diameter and intensity varied less than 5%, when stored at 4 °C. Data were reported as the mean of five measurements of three different vesicles' preparations.

Enzymatic activity measurements

For ATP hydrolysis, phosphomonohydrolase activities were assayed discontinuously by measuring the amount of released P_i at 37 °C in 50 mM Tris–HCl buffer containing 2 mM $MgCl_2$, pH 7.4, as previously described [24, 26]. One enzyme unit (1 U/mg) is defined as the amount of enzyme hydrolyzing 1.0 nmol of substrate per minute per milligram of

protein. Maximum velocity (V_{max}), apparent dissociation constant ($K_{0.5}$), and Hill coefficient (n) obtained from substrate hydrolysis were calculated as described [33]. Data were reported as the mean of triplicate measurements of three different enzyme preparations. Statistically significant differences were defined as $p < 0.05$.

Synthesis of ACP and PS-CPLX nucleators

ACP and PS-CPLX nucleators were synthesized as previously described [3, 34, 35].

Mineralization assays with proteoliposomes

TNAP-proteoliposomes were incubated in SCL buffer in the presence or absence of ACP or PS-CPLX at pH 7.5. SCL contained 2 mM Ca^{2+}, 104.5 mM Na^+, 133.5 mM Cl^-, 63.5 mM sucrose, 16.5 mM Tris, 12.7 mM K^+, 5.55 mM glucose, 1.83 mM HCO_3^-, and 0.57 mM $MgSO_4$ [34]. The assay was accomplished with a saturating ATP concentration (as the P_i source) for TNAP activity present in each distinct proteoliposome. Thus, ATP concentrations of 6 mM, 10 mM, 5 mM, and 9 mM were used for the proteoliposomes composed of DPPC, DPPC:Chol (9:1), DPPC:SM (9:1), and DPPC:Chol:SM (8:1:1), respectively. Enzyme-devoid liposomes were used as control. Mineral formation/propagation was measured by turbidity at 340 nm (A_{340}) using a multi-well microplate assay as described before [34]. Triplicate samples (280 μL) were successively distributed into wells of a 96-well microplate. Turbidity measurements were made after brief agitation (10 s) followed by 48 h of incubation at 37 °C, using a Molecular Devices M3 microplate reader (Sunnyvale, CA). The results were normalized according to the protein concentration of each proteoliposome, since different efficacies of TNAP incorporation were obtained depending on the lipid composition of the proteoliposome.

Fourier-transform infrared spectroscopy

The proteoliposomes were incubated in SCL buffer, as described above, in the absence of nucleators. Then, the samples were placed on the germanium crystal of an attenuated total reflectance (ATR) accessory to assess the chemical groups in the formed minerals by means of FTIR spectroscopy (Shimadzu-IRPrestige-21). The efficacy of mineralization was assessed by calculating the ratio between the areas of the internal reference band of the ester phospholipid (C=O) at 1740 cm^{-1} and the band corresponding to the asymmetrical stretching of the PO_4^{3-} group at 1032 cm^{-1}.

Statistical analysis

All quantitative measurements were carried out 3–5 times and values are reported as mean ± standard error of the mean (SEM). Groups were compared with the one-way ANOVA or a two-tailed Student's t test. A p value of < 0.05 was considered significant.

Results

Biomineralization induced by MVs is a complex process in which Ca^{2+} and P_i accumulate inside MVs and induce nucleation and formation of apatitic minerals [5, 7]. Previously, we have characterized the incorporation of TNAP into proteoliposomes made of DPPC:Chol, DPPC:SM, or DPPC:Chol:SM by differential scanning calorimetry (DSC) [30]. Here, the

biophysical characterization of vesicles by DLS (Table 1) showed that the average diameters of the liposomes and proteoliposomes did not alter significantly when compared with the diameter obtained for DPPC-vesicles. Comparing the sizes distribution of liposomes with proteoliposomes harboring TNAP, in the presence of TNAP, no more than 10% in the increase in the vesicles diameter was observed (DPPC-vesicles 6%, DPPC:Chol-vesicles 10%, DPPC:SM-vesicles 6% and DPPC:Chol:SM-vesicles 4%) (Table 1). Comparing the lipid compositions in the presence of cholesterol and sphingomyelin with neat DPPC-vesicles, the diameter of vesicles formed did not alter significantly (maximum variation of 15%), despite the diverse lipid compositions studied. Low polydispersity index (PI) values were obtained for the different lipids compositions, indicating that the samples were nearly monodisperse in size (Table 1).

The kinetic behavior of membrane-anchored TNAP depends on the lipid composition of the liposomes [26]. Thus, we have investigated the effect of the liposome composition on the kinetic parameters of the reconstituted TNAP 1:10,000 protein:lipid (molar ratio), to determine the saturating ATP concentration for each lipidic composition, as shown by the arrows in Fig. 1. For DPPC-proteoliposomes harboring TNAP, V_{max} values were observed to follow the order DPPC:Chol (9:1) > DPPC:SM (9:1) > DPPC:Chol:SM (8:1:1) proteoliposomes (Table 2). Only positive cooperativity (n) was observed for ATP hydrolysis for all tested compositions (Table 2). The catalytic efficiencies of DPPC, DPPC:Chol (9:1), and DPPC:SM (9:1) showed the same order of magnitude (from 5.7×10^2 to 3.5×10^2 M^{-1} s^{-1}) and a lower value was obtained for the ternary composition (1.1×10^1 M^{-1} s^{-1}) (Table 2).

We then assessed the ability of these proteoliposomes to induce/propagate biomineralization in a SCL buffer with a saturating ATP concentration (as a source of P_i) for TNAP activity present in each distinct proteoliposome, and in the presence or absence of ACP or PS-CPLX as nucleators. Thus, ATP concentrations of 6 mM, 10 mM, 5 mM, and 9 mM were used for the proteoliposomes composed of DPPC, DPPC:Chol (9:1), DPPC:SM (9:1), and DPPC:Chol:SM (8:1:1), respectively, as determined in Fig. 1.

We found that DPPC-proteoliposomes induced mineral formation, as probed by turbidity assay, when incubated for 48 h in SCL buffer containing saturating concentration of ATP as TNAP substrate (Fig. 2). DPPC:Chol (9:1), DPPC:SM (9:1), and DPPC:Chol:SM (8:1:1) (Fig. 2) proteoliposomes harboring TNAP produced less mineral than DPPC-proteoliposomes. DPPC:Chol:SM-proteoliposomes induced slightly less minerals than those produced by DPPC:SM-proteoliposomes, however, higher than those produced by DPPC:Chol-proteoliposomes.

Notably, the presence or absence of a nucleator (ACP or PS-CPLX) did not significantly affect the production of minerals in any of the proteoliposomes.

The differences in mineralization efficiency among the distinct types of proteoliposomes were further assessed by means of ATR-FTIR spectroscopy (Fig. 3). Indeed, turbidity did not provide the nature of mineral formed, therefore we used IR spectroscopy to determine the type of minerals. This analysis was performed in the absence of nucleator. All the

recorded ATR-FTIR spectra showed broad bands at 3470–3410 cm^{-1} that were assigned to the O–H stretching vibrations of water [36]. The sharp and strong absorption bands at 2922 and 2852 cm^{-1} were assigned to the asymmetric and symmetric, respectively, C–H stretching vibrations of the CH$_2$ groups of acyl chains. The band of the ester carbonyl C=O group of phospholipids was located at 1740 cm^{-1}, whereas the C–H scissoring band was at 1470 cm^{-1}. The C–O vibration characteristic of fatty acid esters generated a band at 1234 cm^{-1}, whereas in the 1090–960 cm^{-1} regions were located the broad absorption bands arising from the P–O stretches of both organic and inorganic phosphate [37]. The latter bands confirmed that a phosphate mineral phase arose after incubating the vesicles in SCL buffer with ATP, validating that the proteoliposomes were able to induce mineralization even in the absence of a nucleator.

To get more quantitative information about the difference in the apatite minerals produced by the different types of proteoliposomes, we calculated the ratios between the area of the FTIR band relative to the apatite minerals at ~ 1032 cm^{-1} and that of the band relative to carbonyl group of the phospholipids at ~ 1740 cm^{-1} (Table 3). These data showed that DPPC-proteoliposomes harboring TNAP without Chol induced the formation of minerals more effectively than the vesicles containing this sterol and that the ternary system produced more minerals than the binary systems, thus validating the results obtained through the turbidity assay (Fig. 3b).

Discussion

The lipid composition of MVs is different from that of the plasma membrane and from the total lipid composition in the whole cell [38, 39]. The main differences are a greater amount of PS (3.2–4.5 fold), SM (2.2–2.5 fold), and total lysophospholipids (1.8–2.2 fold), and a smaller amount of PC (0.6–0.7 fold) in MVs with respect to whole cells. Additionally, MVs are enriched in Chol and depleted in triacylglycerols compared to the plasma membrane and whole cells [20, 39]. The activity of membrane enzymes is affected by the lipid microenvironment [23, 30, 40–42]. We have previously described that an increase in the complexity of the proteoliposomes decreased the activity of GPI-anchored TNAP incorporated in the membrane [30]. Herein, we investigated the effects of the lipid composition on the ability of proteoliposomes to produce apatite minerals by means of turbidity assay. We found that proteoliposomes produced minerals in the order DPPC > DPPC:SM (9:1) > DPPC:Chol:SM (8:1:1) > DPPC:Chol (9:1) proteoliposomes, probably due to the lipid phase behavior of the membrane microenvironments [30, 40], which can influence differently the V_{max} of ATP hydrolysis and catalytic efficiency of TNAP, as observed in Table 2. Studies regarding biomineralization comparing other sources of P$_i$ for TNAP hydrolysis when incorporated in proteoliposomes are need to be performed. However, the scenario with PP$_i$, for example, is even more complex than ATP. Beyond substrate, PP$_i$ is a potent inhibitor of TNAP activity and can also suppress hydroxyapatite crystal formation and propagation acting as a potent calcification inhibitor in biologic fluids [4].

Chol alters the physical properties and lateral organization of the plasma membrane by increasing the thickness and decreasing the permeability of the phospholipid bilayer [29, 30, 40, 43–45]. Addition of Chol decreases the area occupied per molecule in lipid bilayers,

which increases lipid/lipid interactions and induces a separation of membrane lipids into a fluid liquid crystalline phase (Lα) and a liquid ordered phase (Lo) enriched in Chol and sphingolipids [17, 30, 40, 43]. The presence of Lo microdomains in proteoliposomes may explain the lower levels of minerals generated by Chol-containing proteoliposomes compared to Chol-devoid ones (Fig. 2).

The DPPC:SM membranes form distinct types of clusters than DPPC:Chol membranes [44, 45]. In particular, DPPC:SM vesicles did not display lateral phase segregation on the membrane as observed on DPPC liposomes [30], which may explain the higher levels of mineral produced by proteoliposomes made of DPPC and DPPC:SM (9:1) when compared to those made in the presence of Chol (DPPC:Chol and DPPC:Chol:SM) (Fig. 2). Finally, the insertion of SM in the DPPC:Chol system stabilizes the membrane through hydrogen bridges between the hydrocarbon chains, which may explain the increased levels of mineral formation observed in DPPC:Chol:SM (8:1:1) proteoliposomes compared to DPPC:Chol (9:1) ones (Fig. 2).

The infrared spectra of all proteoliposomes displayed the band relative to the apatite minerals centered at ~ 1032 cm^{-1}, which confirmed that minerals were produced by all the lipidic systems. Additionally, the values of the ratio between the area of the apatite band at ~ 1032 cm^{-1} and that of the phospholipid-specific band at ~ 1740 cm^{-1} (ester carbonyl C=O) for the tested proteoliposomes was higher for pure DPPC-TNAP compared to the proteoliposomes containing Chol and SM [46]. This result further validated that the proteoliposomes without Chol induced mineral formation more efficiently than those containing Chol.

In conclusion, we found that proteoliposomes harboring TNAP have the ability to induce mineralization after 48 h of incubation under saturating ATP concentrations as the source of P_i, even in absence of a nucleator. Additionally, we found that the presence of ordered domains due to the addition of Chol to DPPC or DPPC:SM-proteoliposomes decreased their ability to produce minerals. Our results indicated that in addition to the essential components required for the mineralization, such as enzymes, substrates, ions and lipids, the degree of packaging of lipid bilayers can affect the phosphohydrolytic activity and catalytic efficiency of TNAP in the bilayers, as well as affecting the supersaturation conditions necessary to precipitate apatite crystals. The diameter of vesicles formed did not alter significantly, despite the diverse lipid compositions studied. Thus, the physical properties and the lateral-phase organization of lipids in proteoliposomes are relevant to regulate the apatite propagation mediated by TNAP function during mineralization.

In the future, these proteoliposomes may act as nanodelivery systems mimicking the MVs' function and thus facilitate the bone fractures' regeneration, help the dental implant fixation or decrease the time for patient recovery.

Acknowledgements

References

1. Boskey AL (2006) Mineralization, structure and function of bone. In: Seibel MJ, Robins SP, Biezikian JP (eds) Dynamics of bone and cartilage metabolism Academic Press, San Diego, pp 201–212

2. Wu LN, Yoshimori T, Genge BR, Wu LN, Yoshimori T, Genge BR, Sauer GR, Kirsch T, Ishikawa Y, Wuthier RE (1993) Characterization of the nucleational core complex responsible for mineral induction by growth plate cartilage matrix vesicles. J Biol Chem 268(33):25084–25094 [PubMed: 8227072]

3. Wu LN, Genge BR, Dunkelberger DG, LeGeros RZ, Concannon B, Wuthier RE (1997) Physicochemical characterization of the nucleational core of matrix vesicles. J Biol Chem 272(7): 4404–4411 [PubMed: 9020163]

4. Millán JL (2013) The role of phosphatases in the initiation of skeletal mineralization. Calcif Tissue Int 93:299–306 [PubMed: 23183786]

5. Bottini M, Mebarek S, Anderson KL, Strzelecka-Kiliszek A, Bozycki L, Simao AMS, Bolean M, Ciancaglini P, Pikula JB, Pikula S, Magne D, Volkmann N, Hanein D, Millan JL, Buchet R (2018) Matrix vesicles from chondrocytes and osteoblasts: Their biogenesis, properties, functions and biomimetic models. Biochim Biophys Acta Gen Subj 1862(3):532–546 [PubMed: 29108957]

6. Ali SY, Sajdera SW, Anderson HC (1970) Isolation and characterization of calcifying matrix vesicles from epiphyseal cartilage. Proc Natl Acad Sci USA 67:1513–1520 [PubMed: 5274475]

7. Robison R (1923) The possible significance of hexosephosphoric esters in ossification. Biochem J 17:286–293 [PubMed: 16743183]

8. Meyer JL (1984) Can biological calcification occur in the presence of pyrophosphate? Arch Biochem Biophys 231:1–8 [PubMed: 6326671]

9. Rezende AA, Pizauro JM, Ciancaglini P, Leone FA (1994) Phosphodiesterase activity is a novel property of alkaline phosphatase from osseous plate. Biochem J 301(Pt 2):517–522 [PubMed: 8042997]

10. Fleisch H, Bisaz S (1962) Mechanism of calcification: inhibitory role of pyrophosphate. Nature 195:911

11. Hsu HH, Camacho NP, Anderson HC (1999) Further characterization of ATP-initiated calcification by matrix vesicles isolated from rachitic rat cartilage. Membrane perturbation by detergents and deposition of calcium pyrophosphate by rachitic matrix vesicles. Biochim Biophys Acta 1416:320–332 [PubMed: 9889389]

12. Ciancaglini P, Yadav MC, Simao AM, Narisawa S, Pizauro JM, Farquharson C, Hoylaerts MF, Millan JL (2010) Kinetic analysis of substrate utilization by native and TNAP-, NPP1-, or PHOS-PHO1-deficient matrix vesicles. J Bone Miner Res 25(4):716–723 [PubMed: 19874193]

13. Simao AM, Yadav MC, Ciancaglini P, Millan JL (2010) Proteoliposomes as matrix vesicles' biomimetics to study the initiation of skeletal mineralization. Braz J Med Biol Res 43(3):234–241 [PubMed: 20401430]

14. Yadav MC, Bottini M, Cory E, Bhattacharya K, Kuss P, Narisawa S, Sah RL, Beck L, Fadeel B, Farquharson C, Millan JL (2016) Skeletal Mineralization Deficits and Impaired Biogenesis and Function of Chondrocyte-Derived Matrix Vesicles in Phospho1(−/−) and Phospho1/Pi t1 Double-Knockout Mice. J Bone Miner Res 31(6):1275–1286 [PubMed: 26773408]

15. Ciancaglini P, Simao AM, Camolezi FL, Millan JL, Pizauro JM (2006) Contribution of matrix vesicles and alkaline phosphatase to ectopic bone formation. Braz J Med Biol Res 39(5):603–610 [PubMed: 16648897]

16. Simons K, Coskun U, Grzybek M, Lingwood D, Levental I, Kaiser HJ (2010) Lipid-protein interactions governing raft partitioning in membranes. Chem Phys Lipids 163:S10–S10

17. Lingwood D, Simons K (2010) Lipid rafts as a membrane-organizing principle. Science 327:46–50 [PubMed: 20044567]

18. Wu LN, Genge BR, Kang MW, Arsenault AL, Wuthier RE (2002) Changes in phospholipid extractability and composition accompany mineralization of chicken growth plate cartilage matrix vesicles. J Biol Chem 277(7):5126–5133 [PubMed: 11714705]

19. Bolean M, Simao AMS, Barioni MB, Favarin BZ, Sebinelli HG, Veschi EA, Janku TAB, Bottini M, Hoylaerts MF, Itri R, Millan JL, Ciancaglini P (2017) Biophysical aspects of biomineralization. Biophys Rev 9(5):747–760 [PubMed: 28852989]

20. Balcerzak M, Radisson J, Azzar G, Farlay D, Boivin G, Pikula S, Buchet R (2007) A comparative analysis of strategies for isolation of matrix vesicles. Anal Biochem 361(2):176–182 [PubMed: 17194438]

21. Damek-Poprawa M, Golub E, Otis L, Harrison G, Phillips C, Boesze-Battaglia K (2006) Chondrocytes utilize a cholesterol-dependent lipid translocator to externalize phosphatidylserine. Biochemistry 45(10):3325–3336 [PubMed: 16519527]

22. Ciancaglini P, Simao AMS, Bolean M, Millan JL, Rigos CF, Yoneda JS, Colhone MC, Stabeli RG (2012) Proteoliposomes in nanobiotechnology. Biophys Rev 4(1):67–81 [PubMed: 28510001]

23. Simao AM, Yadav MC, Narisawa S, Bolean M, Pizauro JM, Hoylaerts MF, Ciancaglini P, Millan JL (2010) Proteoliposomes harboring alkaline phosphatase and nucleotide pyrophosphatase as matrix vesicle biomimetics. J Biol Chem 285(10):7598–7609 [PubMed: 20048161]

24. Simao AM, Bolean M, Hoylaerts MF, Millan JL, Ciancaglini P (2013) Effects of pH on the production of phosphate and pyrophosphate by matrix vesicles' biomimetics. Calcif Tissue Int 93(3):222–232 [PubMed: 23942722]

25. Simao AMS, Bolean M, Cury TAC, Stabeli RG, Itri R, Ciancaglini P (2015) Liposomal systems as carriers for bioactive compounds. Biophys Rev 7(4):391–397 [PubMed: 28510100]

26. Bolean M, Simao AM, Kiffer-Moreira T, Hoylaerts MF, Millan JL, Itri R, Ciancaglini P (2015) Proteoliposomes with the ability to transport Ca(2+) into the vesicles and hydrolyze phosphosubstrates on their surface. Arch Biochem Biophys 584:79–89 [PubMed: 26325078]

27. Bolean M, Borin IA, Simao AMS, Bottini M, Bagatolli LA, Hoylaerts MF, Millan JL, Ciancaglini P (2017) Topographic analysis by atomic force microscopy of proteoliposomes matrix vesicle mimetics harboring TNAP and AnxA5. Biochim Biophys Acta 1859(10):1911–1920

28. Itel F, Skovhus Thomsen J, Städler B (2018) Matrix vesicles-containing microreactors as support for bone-like osteoblast cells to enhance biomineralization. ACS Appl Mater Interfaces 10.1021/acsami.8b10886

29. Bolean M, Simao AM, Favarin BZ, Millan JL, Ciancaglini P (2010) The effect of cholesterol on the reconstitution of alkaline phosphatase into liposomes. Biophys Chem 152(1–3):74–79 [PubMed: 20810204]

30. Bolean M, Simao AM, Favarin BZ, Millan JL, Ciancaglini P (2011) Thermodynamic properties and characterization of proteoliposomes rich in microdomains carrying alkaline phosphatase. Biophys Chem 158(2–3):111–118 [PubMed: 21676530]

31. Simao AM, Beloti MM, Cezarino RM, Rosa AL, Pizauro JM, Ciancaglini P (2007) Membrane-bound alkaline phosphatase from ectopic mineralization and rat bone marrow cell culture. Comp Biochem Physiol A Mol Integr Physiol 146(4):679–687 [PubMed: 16798036]

32. Hartree EF (1972) Determination of protein: a modification of the Lowry method that gives a linear photometric response. Anal Biochem 48:422–427 [PubMed: 4115981]

33. Leone FA, Baranauskas JA, Furriel RP, Borin IA (2005) SigrafW: An easy-to-use program for fitting enzyme kinetic data. Biochem Mol Biol Educ 33(6):399–403 [PubMed: 21638609]

34. Genge BR, Wu LN, Wuthier RE (2007) In vitro modeling of matrix vesicle nucleation: synergistic stimulation of mineral formation by annexin A5 and phosphatidylserine. J Biol Chem 282:26035–26045 [PubMed: 17613532]

35. Wuthier RE, Chin JE, Hale JE, Register TC, Hale LV, Ishikawa Y (1985) Isolation and characterization of calcium-accumulating matrix vesicles from chondrocytes of chicken epiphyseal growth plate cartilage in primary culture. J Biol Chem 260(29):15972–15979 [PubMed: 3905800]

36. Ishikawa T, Wakamura M, Kondo S (1989) Surface characterization of calcium hydroxylapatite by Fourier transform infrared spectroscopy. Langmuir 5:140–144

37. Fowler BO, Markovic M, Tung MS (2004) Preparation and comprehensive characterization of a calcium hydroxyapatite reference material. J Res Natl Inst Stand Technol 109:553–568 [PubMed: 27366634]

38. Peress NS, Anderson HC, Sajdera SW (1974) The lipids of matrix vesicles from bovine fetal epiphyseal cartilage. Calcif Tissue Res 14:275–281 [PubMed: 4367314]

39. Wuthier RE, Lipscomb GF (2011) Matrix vesicles: structure, composition, formation and function in calcification. Front Biosci 16:2812–2902

40. Favarin BZ, Andrade MAR, Bolean M, Simao AMS, Ramos AP, Hoylaerts MF, Millan JL, Ciancaglini P (2017) Effect of the presence of cholesterol in the interfacial microenvironment on the modulation of the alkaline phosphatase activity during in vitro mineralization. Colloids Surf B Biointerfaces 155:466–476 [PubMed: 28472750]

41. Lehto MT, Sharom FJ (2002) Proximity of the protein moiety of a GPI-anchored protein to the membrane surface: a FRET study. Biochemistry 41:8368–8376 [PubMed: 12081485]

42. Sesana S, Re F, Bulbarelli A, Salerno D, Cazzaniga E, Masserini M (2008) Membrane features and activity of GPI-anchored enzymes: alkaline phosphatase reconstituted in model membranes. Biochemistry 47(19):5433–5440 [PubMed: 18416535]

43. Simons K, Ikonen E (1997) Functional rafts in cell membranes. Nature 387:569–572 [PubMed: 9177342]

44. Brown DA, London E (2000) Structure and function of sphingolipid- and cholesterol-rich membrane rafts. J Biol Chem 275:17221–17224 [PubMed: 10770957]

45. Snyder B, Freire E (1980) Compositional domain structure in phosphatidylcholine-cholesterol and sphingomyelin-cholesterol bilayers. Proc Natl Acad Sci USA 77:4055–4059 [PubMed: 6933455]

46. Cheng ZH, Yasukawa A, Kandori K, Ishikawa T (1998) FTIR study of adsorption of CO_2 on nonstoichiometric calcium hydroxyapatite. Langmuir 14(23):6681–6686
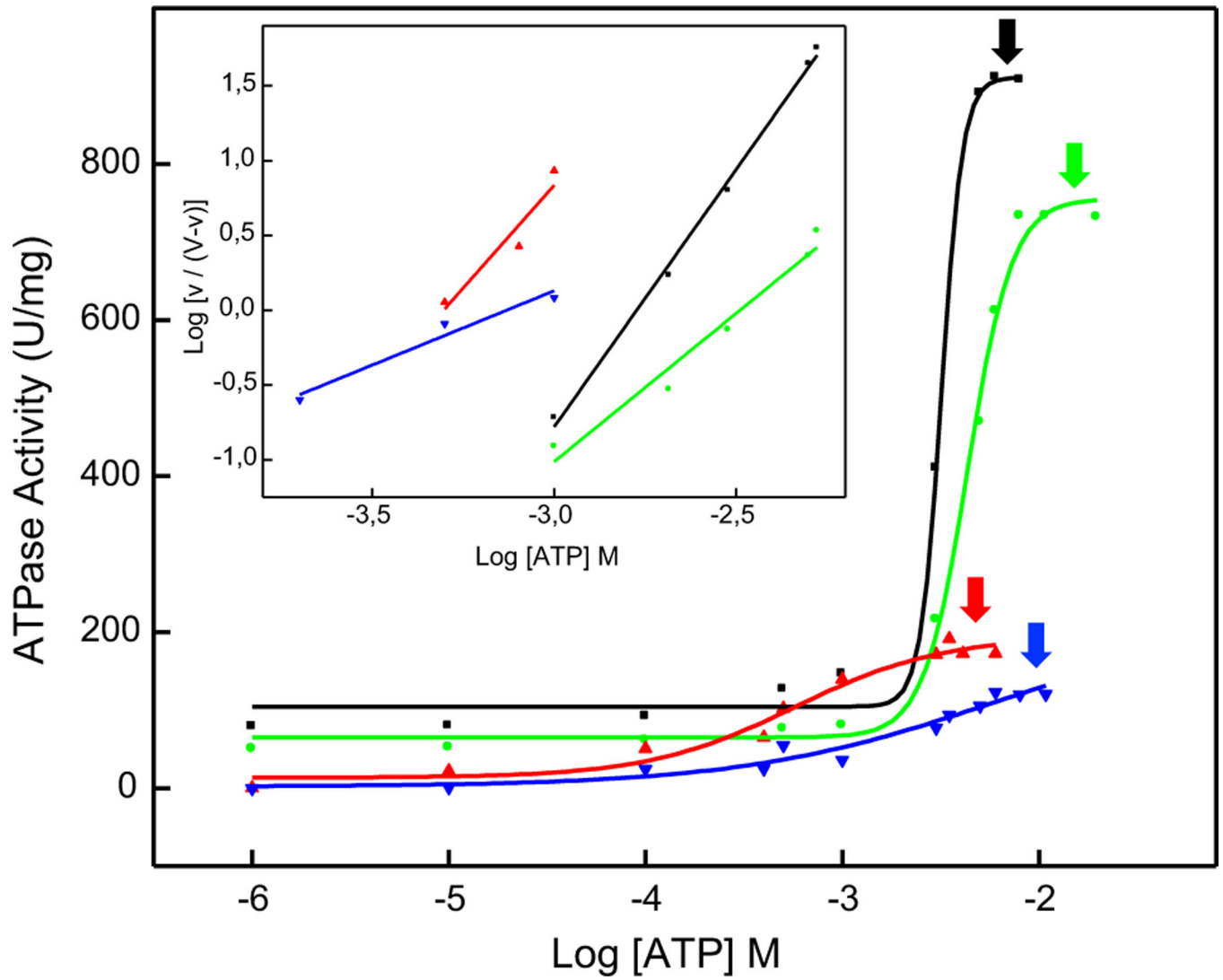
Fig. 1.
Achievement of V_{max} for the hydrolysis of ATP by TNAP-proteoliposomes composed of different lipid compositions: (black) DPPC, (green) DPPC:Chol (9:1), (red) DPPC:SM (9:1) and (blue) DPPC:Chol:SM (8:1:1) (molar ratios). Arrows indicate the saturating ATP concentration for each distinct proteoliposome. Inset: representation to determine Hill coefficient (*n*). Data were reported as the mean of triplicate measurements of three different enzyme preparations
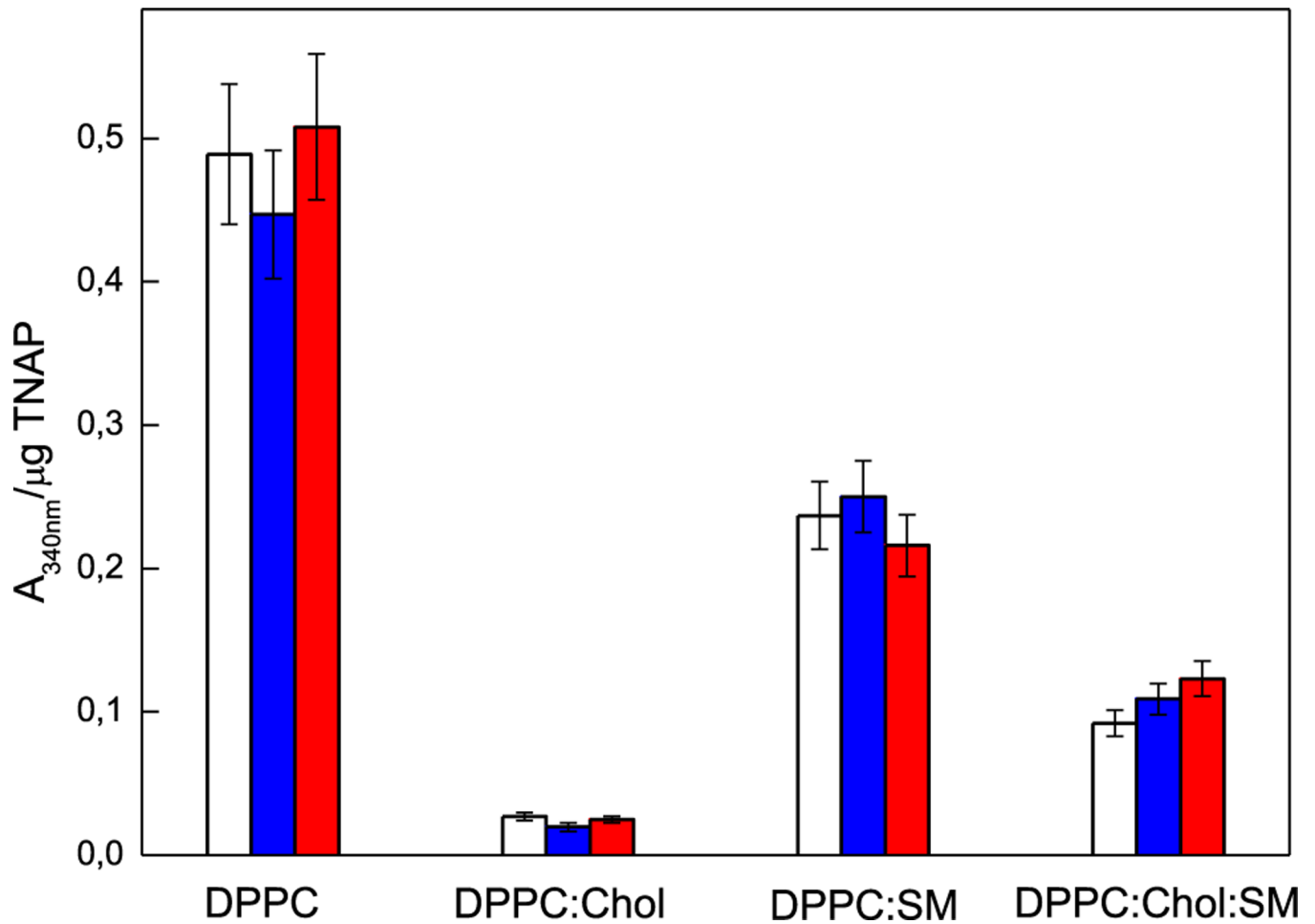
Fig. 2.
Effect of TNAP-proteoliposomes composed of DPPC, DPPC:Chol (9:1), DPPC:SM (9:1) and DPPC:Chol:SM (8:1:1) (molar ratios), on mineral propagation in the absence of nucleator (blank) and in the presence of ACP (blue) or PS-CPLX-seeded SCL (red), at pH 7.5. The assay was accomplished in SCL buffer with a saturating ATP concentration for TNAP activity for each distinct proteoliposome. ATP concentrations of 6 mM, 10 mM, 5 mM, and 9 mM were used for the proteoliposomes composed of DPPC, DPPC:Chol, DPPC:SM and DPPC:Chol:SM, respectively, as indicated by arrows in Fig. 1. Enzyme-devoid liposomes were used as control and bars show the increment in absorbencies after 48 h of incubation at 37 °C. All results are expressed as mean ± SEM. $P < 0.05$
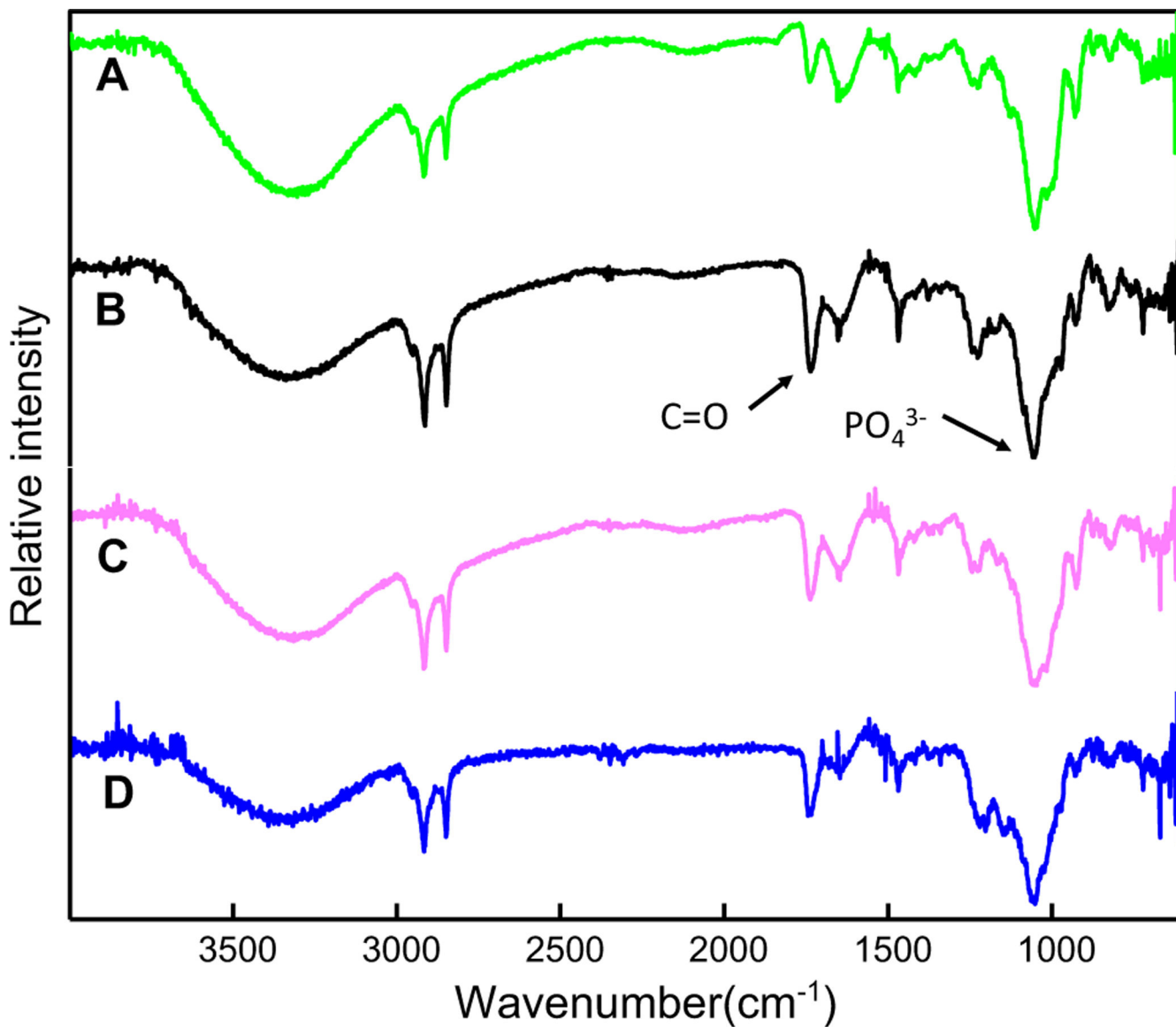
Fig. 3.
FTIR spectra of the minerals obtained from the mineralization assays under incubation of TNAP-proteoliposomes composed of (green) DPPC, (black) DPPC:Chol (9:1), (pink) DPPC:SM (9:1) and (blue) DPPC:Chol:SM (8:1:1) (molar ratios), in SCL, at 37 °C, at pH 7.5, in the absence of nucleators. ATP concentrations of 6 mM, 10 mM, 5 mM, and 9 mM were used for the proteoliposomes composed of DPPC, DPPC:Chol, DPPC:SM and DPPC:Chol:SM, respectively, as indicated by arrows in Fig. 1. Mineralization was followed by the differences in the ratio between the areas of the internal reference band of the phospholipid (C=O) at 1740 cm^{-1} and the band corresponding to the asymmetrical stretching of the PO$_4^{3-}$ group at 1032 cm^{-1}

Table 1

Biophysical characterization by DLS of liposomes and TNAP-proteoliposomes composed by different lipid compositions

Liposome/proteoliposome composition		Diameter (nm)	Polydispersity index (PI)
Lipid (molar ratio)	TNAP		
DPPC	–	115.0 ± 0.4	0.08 ± 0.01
DPPC	+	121.1 ± 5.9	0.15 ± 0.05
DPPC:Chol (9:1)	–	121.9 ± 0.5	0.09 ± 0.03
DPPC:Chol (9:1)	+	133.8 ± 8.8	0.12 ± 0.05
DPPC:SM (9:1)	–	127.1 ± 1.0	0.09 ± 0.03
DPPC:SM (9:1)	+	134.5 ± 9.1	0.09 ± 0.06
DPPC:Chol:SM (8:1:1)	–	133.4 ± 0.8	0.04 ± 0.03
DPPC:Chol:SM (8:1:1)	+	138.8 ± 21.9	0.12 ± 0.11

Table 2

Kinetic parameters for the hydrolysis of ATP by TNAP reconstituted in liposomes 1:10,000 protein:lipid (molar ratio) of different lipid compositions

Kinetic parameters	TNAP-proteoliposomes			
	DPPC	DPPC:Chol	DPPC:SM	DPPC:Chol:SM
$V_{máx}$ (U/mg)	910.0 ± 10.6	732.8 ± 15.3	191.2 ± 12.3	122.8 ± 10.3
$K_{0.5}$ (mM)	3.18 ± 0.02	2.75 ± 0.06	0.32 ± 0.01	2.22 ± 0.04
n	3.42 ± 0.01	1.91 ± 0.07	2.74 ± 0.02	0.99 ± 0.09
$k_{cat}/K_{0.5}$ (M^{-1} s^{-1})	5.7×10^2	5.3×10^2	3.5×10^2	1.1×10^1

Table 3

Ratios between the areas of the bands at 1032 (PO_4^{3-}) and 1740 (C=O) cm^{-1} obtained by ATR-FTIR for the different proteoliposomes samples

Proteoliposomes composition	PO_4^{3-}/C=O
DPPC	3.2 ± 0.1
DPPC:Chol (9:1)	1.8 ± 0.1
DPPC:SM (9:1)	2.2 ± 0.1
DPPC:Chol:SM (8:1:1)	1.9 ± 0.1